SCIENCE CHINA Information Sciences



• LETTER •

January 2026, Vol. 69, Iss. 1, 119402:1–119402:2 https://doi.org/10.1007/s11432-025-4499-6

A 1–10 GHz frequency-agile high-power GaN linear photoconductive semiconductor switch

Xu WANG¹, Xiaoli LU¹*, Ye WANG¹, Ruiqi YANG¹, Xiangjin CHEN², Jingliang LIU², Yunlong HE¹*, Xiaohua MA¹ & Yue HAO¹

 1 School of Microelectronics, Xidian University, Xi'an 710071, China 2 The 13th Research Institute of China Electronics Technology Group Corporation, Shijiazhuang 050051, China

Received 21 February 2025/Revised 25 April 2025/Accepted 12 June 2025/Published online 22 September 2025

Citation Wang X, Lu X L, Wang Y, et al. A 1–10 GHz frequency-agile high-power GaN linear photoconductive semiconductor switch. Sci China Inf Sci, 2026, 69(1): 119402, https://doi.org/10.1007/s11432-025-4499-6

Recently, the advancement of microwave photonics has brought increasing attention to the generation of radio frequency (RF) microwave using laser-modulated linear photoconductive semiconductor switches (PCSSs) [1,2]. SiC stands out due to its high breakdown field, exceptional dark-state resistivity, high electron saturation velocity, and excellent thermal conductivity, making it a prime candidate for developing high-power PCSSs [3]. Xun et al. [4] demonstrated a vertical SiC PCSS achieving a frequencytunable output from 0.5 to 2.5 GHz with a microwave power of 1.36 MW at 1 GHz. Similarly, Chu et al. [5] developed a frequencyagile microwave system based on lateral SiC PCSS, capable of tuning frequencies from 0.5 to 10 GHz and delivering a maximum output power of 1.13 W. In contrast, GaN, another third-generation wide-bandgap semiconductor, offers higher electron mobility and shorter carrier lifetime compared to SiC, theoretically enabling superior frequency response and microwave output. Huang et al. [6] demonstrated that GaN PCSS could achieve a frequency response between 3.3 and 5 GHz with a maximum output power of 1.3 kW with finite element simulation. However, experimental reports on modulated microwave generation using GaN PCSSs remain absent due to the lack of optimization of material composition and device structure. Moreover, the trade-off between operating frequency and output power remains a key limitation for PCSSs in high-frequency applications.

In this study, a 1–10 GHz frequency-agile high-power GaN PCSS was reported for the first time. The design of Fe doping concentration and lateral structure with lower parasitic capacitance ensured high resistivity and high frequency. The shallow trench was additionally introduced to improve the power capacity of the device. Using a 532 nm laser and a 3 kV bias voltage to generate and regulate carrier transport, the device delivered microwave power of 736.3 W at 10 GHz, which is the highest value reported for existing PCSSs.

Experiments. Figure 1(a) shows a lateral GaN PCSS with shallow trench (STPCSS) and its key fabrication process flow. A conventional lateral photoconductive semiconductor switch (CLPCSS) without trenches was also fabricated as a control. Figure 1(b) presents the schematic of the experimental setup for mi-

crowave generation using GaN PCSS. Detailed information on GaN material, device fabrication process, and microwave experimental circuit can be found in Appendixes A and D.

Results and discussion. Fe is introduced to compensate for shallow-level donors (e.g., Si and O) in HVPE GaN. Its concentration can affect photo-generated carrier lifetime, for that Fe deep acceptor energy level could produce an ultrafast capture effect on carriers. The carrier lifetime determines the upper limit of PCSS operating frequency. Therefore, it is crucial to study the effect of Fe doping concentration on the frequency response of GaN PCSS. We use TCAD software to build the STPCSS architecture shown in Figure 1(a). By keeping Si, O doping concentration fixed at 7×10^{17} and 2×10^{16} cm⁻³, Fe concentrations are set to 1×10^{18} , $2\times10^{18},\;4\times10^{18},\;\mathrm{and}\;8\times10^{18}~\mathrm{cm}^{-3}.$ Under 10 GHz laser input, the device output waveforms at different Fe concentrations are shown in Figure 1(c). Results illustrate that with an increase in Fe concentration, the modulation depth gradually increases and the frequency response becomes better. However, the amplitude of the output photocurrent gradually decreases. To balance compensation and excitation efficiency, Fe-doped GaN with a doping concentration of 4×10^{18} cm⁻³ was chosen. Figure 1(d) exhibits the fs-TAS test of the GaN single crystal, revealing a carrier lifetime of 88 ps, which ensures X-band frequency response capability.

Breakdown voltage and the concentration of photo-generated carriers are critical factors affecting PCSS output power. Figure 1(e) shows the dark-state characteristics of the fabricated STPCSS. A picoammeter was employed to measure current under varying bias voltages. High linearity indicates ohmic contact performance. Appendixes B and C provide detailed descriptions of the withstand voltage and ohmic contact of semi-insulating GaN. Figure 1(f) compares the photocurrent performance of STPCSS and CLPCSS under a 1 kV bias and 3 mJ, 1 GHz modulated laser input. The photocurrent of the GaN PCSS increased approximately 22% from 1.45 to 1.77 A. Improvement was attributed to the increased current density, resulting from additional current channels introduced by the trench structure, as evidenced in Figure 1(g).

STPCSS demonstrated superior output performance at 1 $\rm GHz$

 $[\]hbox{* Corresponding author (email: xllu@xidian.edu.cn, ylhe@xidian.edu.cn)}\\$

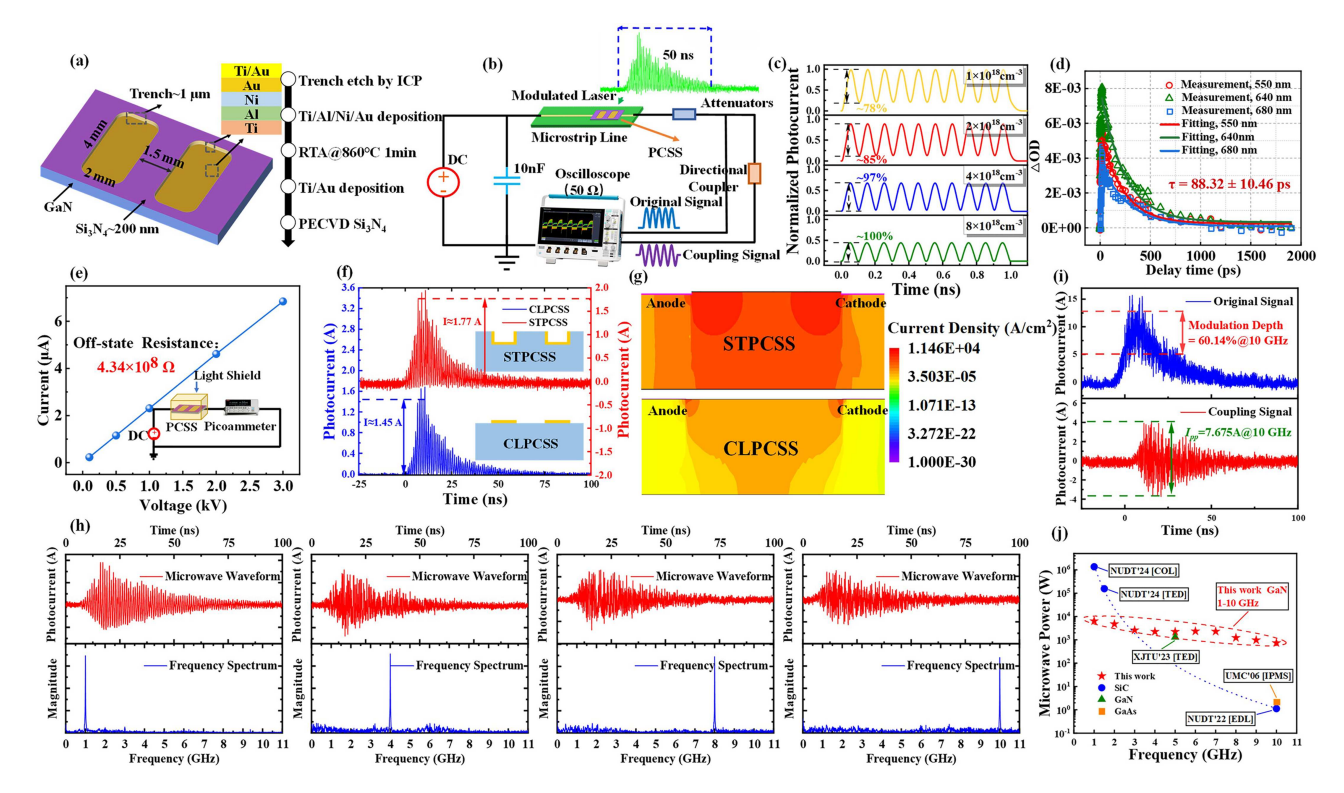


Figure 1 (Color online) (a) Schematic of the STPCSS architecture and process flow; (b) schematic diagram of a photoconductive microwave experimental circuit based on GaN PCSS; (c) normalized photocurrent at different Fe concentrations under 10 GHz laser input; (d) fs-TAS test results and fitting curves; (e) off-state current as a function of bias voltage; (f) comparison of the photocurrent generated by two device structures; (g) current density distribution for the two devices simulated by TCAD; (h) microwave waveforms and spectrum distribution under different frequency trigger lasers; (i) 10 GHz output signals under bias 3 kV and 8 mJ, 10 GHz modulated laser input; (j) benchmark of GaN STPCSS with other linearly modulated PCSSs.

compared to CLPCSS. To explore its potential at higher frequencies, modulated laser signals of 4, 8, and 10 GHz were applied. The output microwave waveforms and frequency spectrum, shown in Figure 1(h), validated the feasibility of frequency-agile microwave generation from 1 to 10 GHz using GaN STPCSS. Increasing the DC bias voltage to 3 kV and modulated laser energy to 8 mJ enabled larger microwave power output at high frequencies. Figure 1(i) displays the original and coupling microwave signals at 10 GHz, with a modulation depth of 60.14% and a peak-topeak current (I_{pp}) of 7.675 A. The microwave output power $(P_{microwave})$ was calculated using the following equation [5] to be 736.3 W:

$$P_{microwave} = (I_{pp}/2)^2 \times R_L, \tag{1}$$

where R_L is the resistance of the load (50 Ω).

Figure 1(j) benchmarks microwave power vs. frequency of our PCSS against previously reported PCSSs. The output power of our device exceeds that of existing linearly modulated PCSSs by two orders of magnitude at 10 GHz. Reasons are that the bias voltage of GaAs PCSS is constrained in linear mode, limiting the output power to the watt range. GaN, as a direct bandgap material, has higher efficiency and mobility compared to SiC. Moreover, a lateral PCSS with a shallow trench not only has lower parasitic capacitance but also improves photocurrent. The relevant description of parasitic parameters is shown in Appendix E. Based on these advantages, GaN STPCSS achieves a balance between output power and microwave frequency.

Conclusion. Through systematic evaluation of carrier lifetime, operating voltage, and photocurrent density, coupled with meticulous optimization of Fe doping concentrations and innovative design of a shallow trench architecture, we have successfully achieved a high-performance GaN linear PCSS. The experimental results of photoelectric response under different modulation frequencies verify the accuracy of the simulation model. A balance between operating frequency and output power further contributes to the record output power of 736.3 W at 10 GHz. This work highlights the potential of GaN PCSS in high-power microwave applications and provides new insights into GaN RF devices.

Acknowledgements This work was supported by National Natural Science Foundation of China (Grant No. 62474133) and Fundamental Research Funds for the Central Universities (Grant Nos. YJSJ24020, QTZX23019).

Supporting information Appendixes A-E. The supporting information is available online at info.scichina.com and link.springer.com. The supporting materials are published as submitted, without typesetting or editing. The responsibility for scientific accuracy and content remains entirely with the authors

References

- Lee C H. Microwave Photonics. Boca Raton: CRC Press, 2013. 3 - 37
- Benford J, Swegle J A, Schamiloglu E. High Power Microwaves. Boca Raton: CRC Press, 2015. 1–12 Sullivan J S, Stanley J R. Wide bandgap extrinsic photoconduc-
- tive switches. IEEE Trans Plasma Sci, 2008, 36: 2528–2532
- Xun T, Niu X, Wang L, et al. Recent progress of parameteradjustable high-power photonic microwave generation based on wide-bandgap photoconductive semiconductors. Chin Opt Lett, 2024, 22: 012501
 Chu X, Xun T, Wang L, et al. Wide-range frequency-
- agile microwave generation up to 10 GHz based on vanadium-compensated 4H-SiC photoconductive semiconductor switch. IEEE Electron Device Lett, 2022, 43: 1013–1016 Huang J, Hu L, Yang X, et al. Modeling and simulation of Fedoped GaN PCSS in high-power microwave. IEEE Trans Electron Devices, 2023, 70: 3489–3495